

The Schrödinger-Langevin equation with and without thermal fluctuations.

R. Katz* and P. B. Gossiaux†

*SUBATECH, Université de Nantes, EMN, IN2P3/CNRS
4 rue Alfred Kastler, 44307 Nantes cedex 3, France*

The Schrödinger-Langevin (SL) equation is considered as an effective open quantum system formalism suitable for phenomenological applications. We focus on two open issues relative to its solutions. We first show that the Madelung/polar transformation of the wavefunction leads to a nonzero friction for the excited states of the quantum subsystem. We then study analytically and numerically the SL equation ability to bring a quantum subsystem to the thermal equilibrium of statistical mechanics. To do so, concepts about statistical mixed states, quantum noises and their production are discussed and a detailed analysis is carried with two kinds of noise and potential.

I. INTRODUCTION

In classical mechanics, the influence of a thermal environment (bath) on a Brownian particle (subsystem) is well described by the phenomenological Langevin dynamics within the Newtonian framework. The subsystem thermalisation is obtained from the balance of two forces (friction and stochastic) which generate irreversible energy exchanges between the two systems. To search for the corresponding description in quantum mechanics has appeared to be crucial for the understanding of quantum fundamentals and in many branches of applied physics (where the quantum systems can never be isolated), such as in microwave cavities [1], quantum diffusion and transport [2, 3], quantum optics [4], heavy ion scattering [5, 6], quantum computers and devices [7–9]... Unfortunately, the Langevin dynamics - or more generally energy dissipation - cannot be introduced easily in the common quantum formalism, as no direct canonical quantization of an Hamiltonian can describe irreversible phenomena [10].

To solve this long standing problem, two main approaches have been proposed and have led to a description of quantum dissipation far from being unique.

1) In the most common approach, the subsystem plus bath is considered as a whole conservative system. Then, by integrating out the bath degrees of freedom, one obtains the dissipative evolution of the subsystem. Generally, this evolution leads to a thermal equilibrium, described by a density matrix, where the energy spectrum components are shifted and

*Electronic address: roland.katz@subatech.in2p3.fr

†Electronic address: Pol-Bernard.Gossiaux@subatech.in2p3.fr

broadened [11]. These spectrum modifications become negligible at the weak coupling limit¹, and one expects the thermal equilibrium predicted by statistical mechanics, i.e. Boltzmann distributions of the uncoupled subsystem energy states. Unfortunately, because in most situations defining the bath is rather complicated and because the calculation is entangled, the application of this approach to phenomenology is not straightforward. Nevertheless, a simple model of the bath [1, 12, 13] - a thermal ensemble of oscillators linearly coupled to the subsystem - has proven to be a suitable framework to study Brownian motion. In the quantum realm and at the weak coupling limit, this model leads to an effective Langevin equation for Heisenberg operators (“HL” equation),

$$\dot{P} = F_{\text{ext}}(X) - AP + F_R(t) \quad \text{and} \quad \dot{X} = P/m, \quad (1.1)$$

which includes a linear friction operator, parameterised by the drag coefficient A (inverse relaxation time), and a quantum thermal fluctuation operator $F_R(t)$. For now, the ability of the HL equation to bring a subsystem to the correct thermal equilibrium has only been demonstrated in the harmonic case [1, 14].

2) Within the second category, many non-standard quantization procedures [7, 15–17] or new frameworks [18–24] have been suggested to overcome the initial subsystem quantization difficulty. Unfortunately, they have led to different dissipative evolution equations.

In the present work, we focus on an effective equation that has arisen from these two approaches, called the Schrödinger-Langevin (“SL”) equation:

$$i\hbar \frac{\partial \psi(x, t)}{\partial t} = \left[H_0 + \hbar A \left(S(x, t) - \int \psi^* S(x, t) \psi dx \right) - x F_R(t) \right] \psi, \quad (1.2)$$

where S is the (real) phase of the wavefunction, chosen according to a prescription which will be discussed in Sec. II A, and H_0 is the isolated-subsystem Hamiltonian

$$H_0 = -(\hbar^2/2m)\nabla^2 + V_{\text{ext}}(x). \quad (1.3)$$

The SL equation can be derived in many ways: within the first approach from an identification with the HL eq. (1.1) [25] and within the second to describe dissipation only [16, 23, 24, 26–28] or to describe a Brownian motion with the additional fluctuating term [7, 21, 29]. The SL equation exhibits interesting properties: unitarity is preserved at all times [24], the uncertainty principle is always satisfied² [30, 31], and the superposition principle is violated due to the nonlinearities. Even though the friction term is nonlinearly (logarithmically) dependent on the wavefunction, it still corresponds to a linear “ohmic” friction (i.e. proportional to the particle velocity). A nonlinear friction can still be obtained by extending the first approach to a nonlinear coupling [33]. Because of its various derivations, its interesting properties and its phenomenological aspect - only the drag A

¹ One is at the weak coupling limit when the subsystem relaxation time is much larger than the typical microscopic interaction time (between the bath components and the subsystem) and than the subsystem natural oscillation time. One then obeys the Brownian hierarchy.

² As opposed to other models like the Caldirola-Kanai equation [18] without fluctuations or the Wigner-Moyal equation with classical Fokker-Planck terms.

and bath temperature T_{bath} are necessary; the use of wavefunctions is convenient -, the SL equation is a solid candidate for the effective study of quantum dissipative systems. However, before considering any actual applications to phenomenology, some questions and issues remain to be explored about its solutions.

The study of the solutions of the SL equation without its stochastic term has been carried in many specific cases: analytically [23, 31, 34–37] and numerically [24, 34, 38–40]. Along these analysis, it has been advocated that the stationary eigenstates of H_0 are also stationary states of the equation [23, 36]. This behaviour is in contradiction with what one would expect from damped quantum systems at first sight [1, 10, 12, 13]. As an answer to this expectation, we will show in Sec. II A how to obtain damping even with these states.

Very few studies of the SL equation solutions have however been carried with an additional driving [30, 42] or stochastic term. Kostin [25] first observed that for a free particle plane wave, the SL and HL equations lead to the same solution. Then, Messer [41] studied the evolution of a Gaussian wavefunction in the free and harmonic potentials. In the free case, he showed that the evolution differs from the HL solution, highlighting that the SL and HL equations are not strictly equivalent. In his calculation, Messer assumed that the SL equation leads to the thermal equilibrium of statistical mechanics - which to our knowledge has never been proven or tested - and used a white quantum noise for the stochastic force, which is questionable. Our main contribution will be to study the ability of the SL equation to bring different 1D subsystems to thermal equilibrium (the one corresponding to the weak coupling limit as described above) using either a white or colored noise.

In the first section of the present paper, we will show how the Madelung transformation leads to friction for any excited eigenstates of H_0 (Sec. II A), discuss the possible thermal fluctuation forces for the SL equation and the numerical method to simulate them (Sec. II B), and the way to obtain mixed state observables from statistics (Sec. II C). In Sec. III A 1, we show analytically that the SL equation brings an initial Gaussian wavepacket (in a harmonic potential) to the thermal equilibrium of statistical mechanics if one uses a specific white quantum noise. Then, following the description of the wavefunction evolution pattern during one noise realisation (Sec. III A 2), we numerically study the SL equation approach to thermal equilibrium, in a harmonic and a linear 1D external potentials, using a white (Sec. III) and a colored (Sec. IV) quantum noise. Though the thermal equilibrium of statistical mechanics is only expected at the weak coupling limit (as explained above), the intermediate and strong regimes are also investigated.

II. FRICTION, QUANTUM NOISES AND MIXED STATES

A. A well defined prescription to obtain eigenstates damping

Though theoretically the fluctuation and dissipation aspects cannot be dissociated, it appears that in some specific studies only the damping is considered [24]. Unfortunately, the dissipative part of the SL eq. (1.2) suffers from ambiguities and needs to be defined properly. Its main non-linear term is the real phase $S(x, t)$, defined by the wavefunction decomposition

$$\psi(x, t) = R(x, t)e^{iS(x, t)}, \quad (2.1)$$

where $R(x, t)$ is the real amplitude. $S(x, t)$ is indeterminate at the wavefunction nodes and multivalued (defined to a 2π modulo).

In the literature [23, 24, 36, 43], the phase $S(\psi)$ for real ψ is commonly prescribed to be zero (and thus continuous at the nodes of ψ) while $R(\psi)$ is taken as a real - *positive or negative* - function. This prescription has led to the conclusion that the stationary eigenstates of H_0 are also stationary states of the SL equation, as the dissipation term identically vanishes. For the sake of describing time-dependent situations, a corresponding prescription has however to be adopted for complex ψ as well. It is easily seen that such an analytical continuation unavoidably has one branch cut in each half complex-plane, both of them starting from the origin. Taking those branch cuts along the imaginary axis leads for instance to

$$S(\psi) = \arctan(\Im(\psi)/\Re(\psi)). \quad (2.2)$$

with finite damping term in the SL equation. Therefore, a small modification of ψ (from real axis to complex plane) leads to a large variation of the associated damping of the quantum state, which is the sign of an ill-defined model.

We propose to use instead the ‘‘polar’’ or ‘‘Madelung’’ prescription, where one defines $R(x, t)$ as the module of the wavefunction, i.e. a real *positive* function. In practice, one could use the local argument of the wavefunction,

$$\text{Arg}(\psi) = \text{atan2}(\Im(\psi), \Re(\psi)), \quad (2.3)$$

to determine $S(x, t)$, but the limitation of its values to a 2π interval illustrated in Fig. 1, would lead to discontinuities of the dissipative term with unphysical effects³. To avoid these, we build the phase $S(x, t)$ step by step,

$$S(x + dx) = S(x) + dS(x) \quad \text{where} \quad dS(x) = \text{Arg}[\psi(x + dx)/\psi(x)], \quad (2.4)$$

starting from an arbitrary space point of reference ‘‘0’’ and get

$$S(j \times dx) = S(0) + \sum_{k=1}^j dS(k \times dx). \quad (2.5)$$

The chosen value of the multivalued $S(0)$ is of no importance thanks to the regulator $-\langle S \rangle$, and can therefore be taken to $\text{Arg}[\psi(0)]$.

The polar prescription leads to singular phase shifts $+\pi$ at the wavefunction nodes as shown for instance in Fig. 2. Not only are these discontinuities theoretically allowed (thanks to the phase indeterminacy at the nodes), but they also have a convenient physical consequence: the stationary eigenstates of H_0 are not stationary states of the SL equation anymore. Indeed, for the excited eigenstates $\{\psi_n\}_{n \geq 1}$ of H_0 the friction term becomes a step potential which generates correlations between eigenstates and results in damping. To show the latter assertions, let us assume that an initial wavefunction $\psi = \sum c_n(0) \psi_n$ is equal to an eigenstate $\psi_{m \geq 1}$, i.e. with $c_n(0) = \delta_{nm}$. The SL equation without the thermal fluctuation term yields,

$$\begin{aligned} \dot{c}_n &= -\frac{i}{\hbar} \langle \psi_n | \hat{H}_0 | \psi \rangle - iA \langle \psi_n | (S - \langle S \rangle) | \psi \rangle \\ &= -\frac{i}{\hbar} E_n c_n - iA \sum_k c_k \int (S - \langle S \rangle) \psi_n^* \psi_k dx. \end{aligned} \quad (2.6)$$

³ The invariance under the multiplication of the wavefunction by a simple phase factor would be broken.

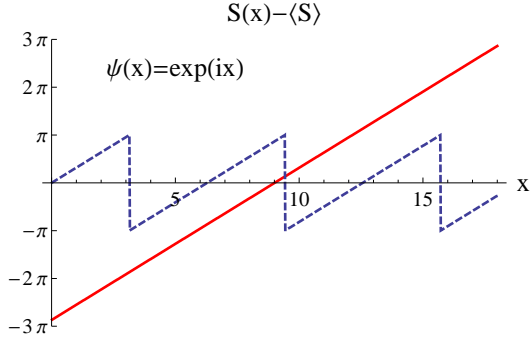


FIG. 1: The dissipative term $S(x) - \langle S \rangle$ corresponding to the plane wave $\psi(x) = e^{ix}$ obtained with the argument function (dashed line) and with the step by step method (solid line).

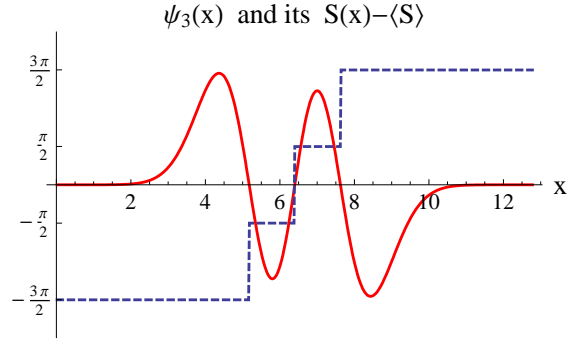


FIG. 2: The real ψ_3 harmonic eigenstate (solid line, magnified for the plot sake) and its corresponding phase $S(x) - \langle S \rangle$ (dashed line) with the step by step method in the polar π prescription.

For symmetric external potentials for instance, one can show that if $\psi_{k=m}$ has an odd (even) parity, then the integral is finite and thus the transition $c_m \rightarrow c_n$ is allowed at very small times for all ψ_n with even (odd) parities. Moreover, the smaller the difference $|n - m|$, the larger the transition rate, which is consistent with the Fermi Golden Rule. Last but not least, the transition to $n = m - 1$ is larger than to $n = m + 1$, which is consistent with damping. At larger times, these transitions and the damping can be observed numerically (see for instance Fig. 3).

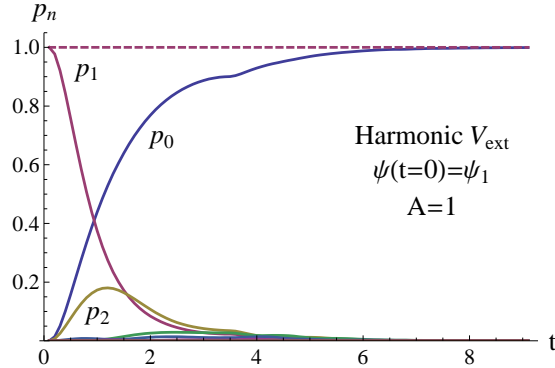


FIG. 3: Evolution of the eigenstate weights $p_{n=0,\dots,10} = |\langle \psi_n | \psi(t) \rangle|^2$ with the dimensionless SL equation (eq. (2.21) without fluctuating term) from an initial first excited state, with the “polar” prescription (solid line) and the “arctan” prescription (dashed line).

Both the “arctan” and “polar” prescriptions are mathematically correct and the choice between them should be physically motivated. Unfortunately, the stationarity of the H_0 eigenstates in the corresponding dissipative situation remains an open question within the open quantum system framework [44]. As illustrated in Fig. 3, thanks to the two prescriptions, the SL equation can reproduce both situations. From our point of view, the polar prescription is however better suited for robust phenomenological studies as we intuitively expect the dissipation to act on any excited state. Let us finally stress that the choice of

the prescription is of little importance when the fluctuations are considered, as they drive the state away from any given eigenstate.

B. Thermal fluctuations and numerical implementation

1. Quantum noises

All the Langevin-like equations include a noise term which simulates the many collisions (or couplings) that the subsystem undergoes with the particles of the bath. This noise is generally taken as a homogeneous Gaussian random process, independent of the subsystem position, and described by its mean and covariance function. The random direction of the many collisions always yields a mean zero. The classical Langevin equation usually assumes no correlation between these collisions, and the white noise covariance writes,

$$\langle F_R(t)F_R(t + \tau) \rangle = 2mkT_{\text{bath}}A \delta(\tau), \quad (2.7)$$

where δ is the Dirac distribution. The asymptotic solution of the Langevin equation is then the corresponding Boltzmann distribution of statistical mechanics.

In the quantum realm, the noise operator is built from the initial bath positions and momentum operators whose non-commutations lead to the main differences with the classical case. Senitzky [1] first proposed an HL equation - for a general bath linearly acting on a harmonic subsystem (with natural frequency ω_0) - where the noise operator is also described by a white covariance,

$$\langle F_R(t)F_R(t + \tau) \rangle = 2mA \left[\frac{\hbar\omega_0}{2} + \frac{\hbar\omega_0}{\exp(\hbar\omega_0/kT_{\text{bath}}) - 1} \right] \delta(\tau). \quad (2.8)$$

This covariance has been used by Messer [41] in its analytic comparison of the HL and SL solutions. The first term of the RHS corresponds to the zero point fluctuations of the subsystem. This term is required within the HL framework for the canonical commutations to hold at $T_{\text{bath}} = 0$, as shown by eq. (52) in [1]. However, within the SL framework, the canonical commutations hold even without fluctuations as the friction goes to zero once the ground state reached. Therefore, this term becomes unnecessary and the white quantum noise writes,

$$\langle F_R(t)F_R(t + \tau) \rangle = B \delta(\tau), \quad (2.9)$$

where $E_0 = 1/2 \hbar\omega_0$ is the zero point energy and

$$B = 2mA E_0 \left[\coth \left(\frac{E_0}{kT_{\text{bath}}} \right) - 1 \right]. \quad (2.10)$$

In Sec. III, we will show that the fluctuation-dissipation relation (2.10) indeed allows to reach an asymptotic thermal distribution of states when one uses a white noise and an external potential.

However, Li et al. [45] pointed out an important weakness in the derivation of (2.8). They also claimed that the colored quantum noise,

$$\langle F_R(t)F_R(t + \tau) \rangle = \frac{m}{\pi} \int_0^\infty \hbar\omega \left[\coth \left(\frac{\hbar\omega}{2kT_{\text{bath}}} \right) \cos(\omega\tau) + i \sin(\omega\tau) \right] A d\omega, \quad (2.11)$$

first derived by Ford et al. [12], is the only one able to drive a general subsystem to the correct thermal equilibrium via the HL equation. For now, the latter assertion has only been demonstrated in a limited form [14, 46].

Actually, in order to get ride of the bath zero point fluctuations contribution - that was first judged physically unjustified -, Ford et al. first derived a quantum noise under the form of the normal product

$$\langle N[F_R(t)F_R(t + \tau)] \rangle = \frac{2mA}{\pi} \int_0^\infty \frac{\hbar\omega}{\exp(\hbar\omega/kT_{\text{bath}}) - 1} \cos(\omega\tau) d\omega. \quad (2.12)$$

As pointed out by Gardiner [46], the correct choice of spectrum depends on what is actually measured to find it: e.g. in absorption measurements one gets the black body radiation Planck spectrum corresponding to (2.12), whereas in Josephson junction noise current measurements [47] one gets the linearly rising spectrum at high frequencies corresponding to (2.11).

Though they are not fully justified (as explained above), we will focus on the white (2.9) and colored (2.12) quantum noise correlations, in order to observe their ability to lead the subsystem toward the thermal equilibrium of statistical mechanics. Our choice not to explore (2.11) within this paper is motivated by the additional complications brought by the required high frequency cut-off, which leads to important model dependences... To use the chosen correlations within the SL framework, we assume that the noise operator can be taken as a commuting c-number (whereas it is usually a non-commuting q-number within the HL framework). Although questionable, this assumption was actually already implied in Kostin's derivation of the SL random potential [25]. Moreover, we note that noise operators as c-numbers have also been derived and studied within the HL framework [48-52].

2. Numerical implementation

To build these noises numerically, we first define a set of uncorrelated Gaussian random variables \hat{r}_j with zero mean and correlation $\langle \hat{r}_j \hat{r}_{j'} \rangle = \Delta t \delta_{jj'}$, where Δt is the time step of the numerical scheme. We build the Gaussian random force \hat{F}_i at a time t_i - and assumed to be constant over the time step $[t_i, t_i + \Delta t]$ - from the weighted sum

$$\hat{F}_i = \sum_{j=-\infty}^{+\infty} W_{i-j} \hat{r}_j, \quad (2.13)$$

where the weights W_{i-j} depend only on the difference $i - j$ to guarantee the stationarity of the process. Then, the mean of \hat{F}_i is null and its covariance is given by

$$\langle \hat{F}_i \hat{F}_{i'} \rangle = \sum_{j,j'=-\infty}^{+\infty} W_{i-j} W_{i'-j'} \langle \hat{r}_j \hat{r}_{j'} \rangle = \sum_{j=-\infty}^{+\infty} W_{i-j} W_{i'-j} \Delta t, \quad (2.14)$$

which, in the continuous limit, becomes

$$\langle F_R(t)F_R(t') \rangle = \int_{-\infty}^{+\infty} W(t-t'') W(t'-t'') dt''. \quad (2.15)$$

Then, one easily shows that the Fourier transform of W is just the square root of the power spectrum $P(\omega)$ of the retained noises, i.e.

$$P(\omega) = 2mA \frac{\hbar\omega}{\exp(\hbar\omega/kT_{\text{bath}}) - 1}, \quad (2.16)$$

for the colored quantum noise (2.12) and

$$P(\omega) = \lim_{\sigma \rightarrow 0} B \exp\left(-\frac{1}{2}\sigma^2\omega^2\right), \quad (2.17)$$

for the white quantum noise (2.9). For the latter, the flat spectrum is obtained when $\sigma \rightarrow 0$, but in practice it is sufficient to take $\sigma \ll \tau$, where τ is the typical time of the subsystem evolution. Then, one gets explicitly

$$W(\tau) = \frac{1}{\pi} \int_0^\infty \sqrt{P(\omega)} \cos(\omega\tau) d\omega. \quad (2.18)$$

In Fig. 4 (left), is shown an example of a colored noise (2.12) realisation obtained with the described numerical method. In Fig. 4 (right), the corresponding numerical correlation over time is successfully compared to the analytical expectation.

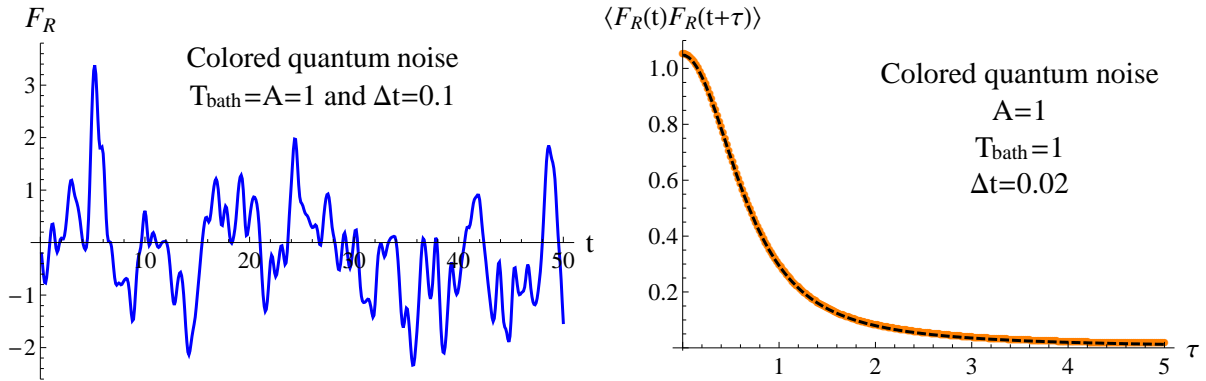


FIG. 4: *Left*: Example of one colored quantum noise (2.12) realisation obtained with the described numerical method. *Right*: Corresponding analytical (dashed black curve) vs. numerical (orange dots) covariances over time.

C. Mixed state observables from statistics

Because of the statistical nature of the bath-subsystem interactions, the subsystem must be described by a mixed state, which includes not only probabilistic information about the observable measurements but also about the state itself. The common tool to describe a mixed state is the density matrix operator,

$$\hat{\rho}(t) = \sum_{n=1}^N p_n(t) |\psi_n\rangle \langle \psi_n|, \quad (2.19)$$

where $\{p_n(t)\}_{n=1,\dots,N}$ is the distribution of the weights of the accessible pure states $\{|\psi_n\rangle\}$. As the SL equation is stochastic and based on a pure state evolution, one needs to perform an average over a large sample of initially identical subsystems to recover the statistical notion implied by the mixed state. The expectation value of an observable operator \hat{O} will then be given by

$$\left\langle \langle \psi(t) | \hat{O} | \psi(t) \rangle \right\rangle_{\text{stat}} = \lim_{n_{\text{stat}} \rightarrow \infty} \frac{1}{n_{\text{stat}}} \sum_{r=1}^{n_{\text{stat}}} \langle \psi^{(r)}(t) | \hat{O} | \psi^{(r)}(t) \rangle, \quad (2.20)$$

where the pure state $|\psi^{(r)}(t)\rangle$ is given by the r^{th} realisation of the stochastic evolution.

The numerical cost will then be proportional to the space-time grid size and to the number of realisations, i.e. to $n_{\text{space}} \times n_{\text{time}} \times n_{\text{stat}}$ (where typically n_{space} is of the order of the hundreds, n_{time} and n_{stat} of the thousands). It remains quite reasonable in comparison to the common density matrix approach where the numerical costs are highly expensive.

D. Dimensionless SL equation

We will study the behaviour of the SL equation with two external potentials: the harmonic $V_{\text{ext}} = 1/2m\omega_0^2 x^2$ and the linear $V_{\text{ext}} = 1/2K_l |x|$. In all the following numerical studies, we use the SL equation with natural units, i.e. $\hbar = m = \omega_0 = K_l = k = 1$, and dimensionless variables x, t, \dots ⁴ Then, the characteristic energies are $E_0 = 1/2\hbar\omega_0 = 0.5$ and $\Delta E = E_1 - E_0 = 1$ ($E_0 \simeq 0.509$ and $\Delta E = E_1 - E_0 \simeq 0.66$) for the harmonic (linear) external potential. The dimensionless SL equation, with the hydrodynamic formulation of the dissipative term, writes

$$i \frac{\partial \psi(x, t)}{\partial t} = \left[\frac{1}{2} \nabla^2 \psi + V_{\text{ext}}(x) + A \left(S(x, t) - \langle S(x, t) \rangle \right) - x F_R(t) \right] \psi, \quad (2.21)$$

where the external potential is $V_{\text{ext}}(x) = 1/2 x^2$ or $V_{\text{ext}}(x) = 1/2 |x|$ within this study. The drag A and the stochastic process are thus the only parameters governing the generic evolution.

III. EQUILIBRATION WITH A WHITE QUANTUM NOISE

A. Harmonic potential

1. Analytic solutions with Gaussian wavepackets as initial conditions

It can be shown that a particular class of solutions for the SL eq. (1.2) is

$$\psi(x, t) = e^{\frac{i}{\hbar} (\alpha(t)[x-x_{\text{cl}}(t)]^2 + p_{\text{cl}}(t)[x-x_{\text{cl}}(t)] + \gamma(t))}, \quad (3.1)$$

⁴ The dimensioned values of x, t, A, F_R and H_0 can be obtained by multiplying our dimensionless values respectively by $\sqrt{\hbar/m\omega_0}, 1/\omega_0, \omega_0, \sqrt{m\hbar\omega_0^3}$ and $\hbar\omega_0$ in the harmonic case or $(\hbar^2/mK_l)^{\frac{1}{3}}, (m\hbar/K_l^2)^{\frac{1}{3}}, (K_l^2/m\hbar)^{\frac{1}{3}}, K_l$ and $(\hbar^2 K_l^2/m)^{\frac{1}{3}}$ in the linear potential case.

where $\alpha(t)$ is a complex number related to the wavepacket width ($\text{Im}(\alpha(t=0)) > 0$), $\gamma(t)$ a complex phase, and x_{cl} and p_{cl} are the position and momentum Gaussian centroids (central values). Inserting (3.1) in the SL equation leads to three ordinary differential equations for α , x_{cl} , p_{cl} and γ , including:

$$\dot{\alpha} + A\text{Re}(\alpha) + \frac{2}{m}\alpha^2 + \frac{m\omega_0^2}{2} = 0 \quad (3.2)$$

and

$$\dot{p}_{\text{cl}} = -m\omega_0^2 x_{\text{cl}} - Ap_{\text{cl}} + F_R, \quad \dot{x}_{\text{cl}} = \frac{p_{\text{cl}}}{m} \quad (3.3)$$

From any $\text{Im}(\alpha(t=0)) > 0$, the solution of eq. (3.2) tends asymptotically to $\alpha(t \rightarrow \infty) = im\omega_0/2$, which corresponds to the width of the ground state $\sqrt{\hbar/m\omega_0}$. After some initial relaxation, the general solution from any initial state (3.1) is thus the ground state displaced in space with a trajectory obeying the classical equations of motion (3.3).

In appendix A we show that the distribution of the eigenstate weights is then the Boltzmann distribution $\propto e^{-E_n/T_{\text{sub}}}$ with $T_{\text{sub}} = T_{\text{bath}}$ (where T_{sub} is the subsystem temperature) provided that the fluctuation-dissipation relation (2.10) is satisfied. In other terms, the subsystem equilibrates with the medium if (2.10) is satisfied. In the following sections, we will show numerically that these results are universal, i.e. independent of the chosen initial state, drag and temperature.

2. Wavefunction pattern during one stochastic realisation

From numerical observations, we first confirm that after some initial relaxation, the general solution from any initial state is the ground state displaced in space with a stochastic trajectory. Indeed with any noises, drags, potentials and initial states, a common wavefunction evolution pattern emerges during a noise realisation (see for instance Fig. 5 and 6). First, as in Sec. III A 1, the shape of the wavefunction evolves toward the ground state shape. In parallel, if one starts from an initial excited eigenstate, the phase “breaks” at the nodes and evolves toward a linear phase in the region where the wavefunction takes non negligible values (see at $t = 17$ in Fig. 6 for instance). In parallel and until the end of the evolution, the centroid oscillates around the potential minimum following a stochastic trajectory along the space axis. Some discrepancies to this pattern, coming from numerical instabilities, appear when $A \ll T$ and when $T \gg 1$.

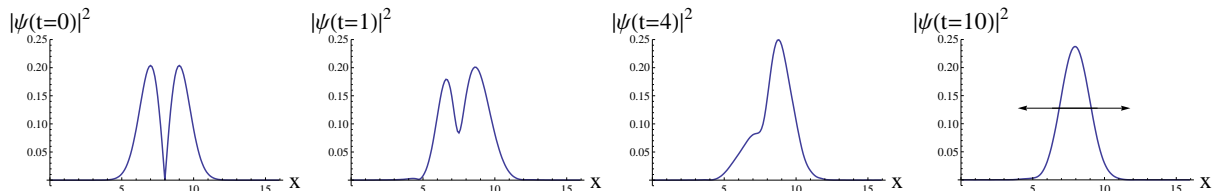


FIG. 5: Typical wavefunction shape/module evolution toward the ground state shape/module during one noise realisation.

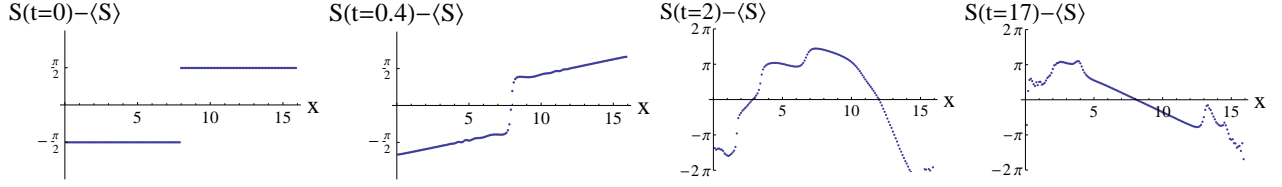


FIG. 6: Typical wavefunction phase evolution towards linearity (where the wavefunction takes significant values) during one noise realisation.

3. Energy and weight evolutions

To illustrate the SL equation ability to bring a subsystem to thermal equilibrium, we choose to evolve the initial ground state ψ_0 in a bath at temperature $T_{\text{bath}} = 1$. The noise parameter is taken as $\sigma = 0.03$ and the grid steps as $\Delta x = 0.1$, $\Delta t = 0.01$.

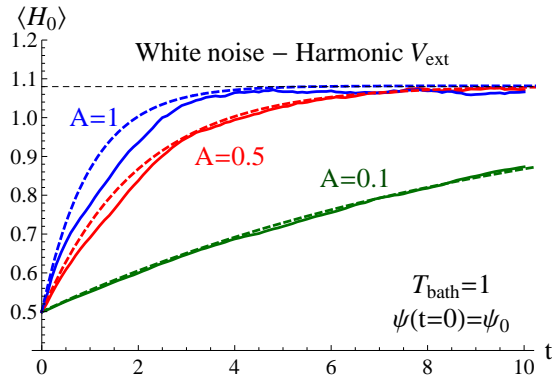


FIG. 7: *Solid curves*: Numerical $\langle H_0 \rangle$ average energy evolutions for different drags A . *Dashed horizontal line*: Corresponding theoretical asymptotic value given by the exact relation (3.4). *Dashed curves*: Corresponding theoretical evolutions given by (3.5).

We first focus on the average energy $\langle\langle H_0 \rangle\rangle_{\text{stat}}$ as given by (2.20); we will just write $\langle H_0 \rangle$ for simplification. Three average energy evolutions with drags corresponding to weak $A = 0.1$, intermediate $A = 0.5$ and strong $A = 1$ couplings (weak coupling if $A \ll \omega_0 = 1$ and $A \ll \sigma$) are shown in Fig. 7. The theoretical asymptotic value for a thermal quantum harmonic oscillator is given by,

$$\langle H_0 \rangle(t \rightarrow \infty) = E_0 \coth \left(\frac{E_0}{kT_{\text{bath}}} \right), \quad (3.4)$$

and corresponds to our value $\langle H_0 \rangle(t \rightarrow \infty) \simeq 1.07$ when $T_{\text{bath}} \simeq 1$. The average energy evolution rate predicted by Senitzsky [1] within the HL equation framework,

$$\langle H_0 \rangle(t) = E_0 e^{-At} + \langle H_0 \rangle(t \rightarrow \infty) (1 - e^{-At}), \quad (3.5)$$

fits our numerical evolution in the weak coupling case (where Senitzsky's HL equation actually applies) as shown in Fig. 7.

The second interesting observable is the distribution of the eigenstate weights (populations) $p_{n=0,\dots,10}(t)$, as given by (2.20) with the projection operator $\hat{O} = |\psi_n\rangle\langle\psi_n|$. As shown

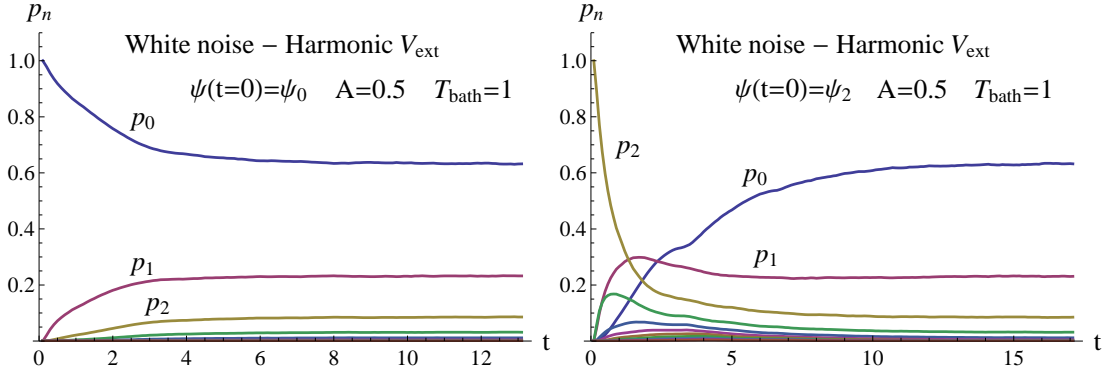


FIG. 8: Evolutions of the eigenstate weights $p_{n=0,\dots,10}(t)$ from the initial ground state (*left*) and 2nd excited state (*right*) for a drag corresponding to an intermediate coupling.

in Fig. 8, their evolutions during the transient phase follow the general expectation of the Fermi Golden Rule: the main transitions occur between neighbouring energy levels. Moreover, they lead to a reshuffling of the weights, such as $p_n > p_{n+1}$, reached after a lapse of time proportional to the relaxation time $1/A$.

4. Asymptotic behaviour

As shown in Fig. 9, the asymptotic distribution of the weights is independent of the chosen initial state and perfectly fits a Boltzmann like distribution. One can determine the *actual temperature reached by the subsystem*, called T_{sub} , by fitting the Boltzmann line $\propto e^{-E/T_{\text{sub}}}$ to the asymptotic $p_{n=0,\dots,10}(E_n)$ values. For the previous example, one finds that $T_{\text{sub}} = 0.99 \simeq T_{\text{bath}}$.

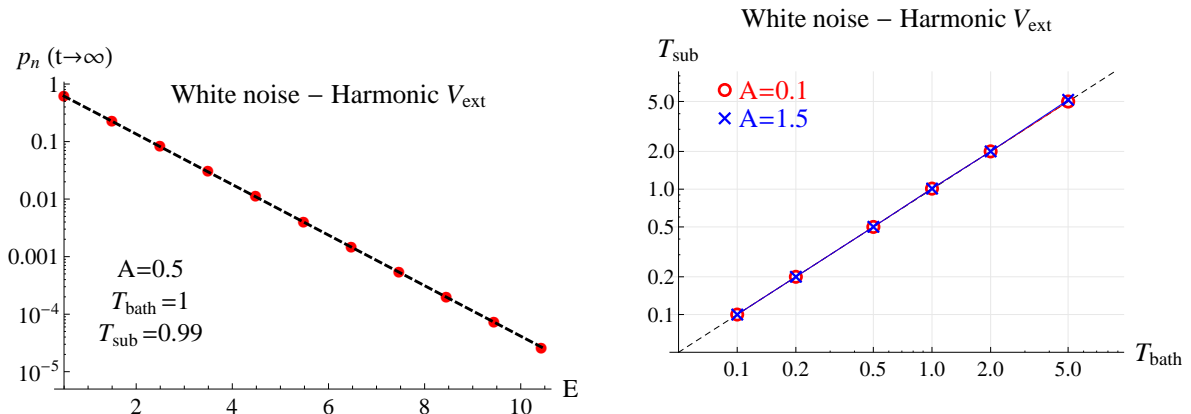


FIG. 9: The asymptotic distribution of the eigenstate weights $p_{n=0,\dots,10}$ (red dots), obtained with $A = 0.5$ and $T_{\text{bath}} = 1$, function of the corresponding eigenenergies $E_{n=0,\dots,10}$. It fits the Boltzmann distribution ($\propto e^{-E/T_{\text{sub}}}$) with $T_{\text{sub}} = 0.99$ (dashed line).

FIG. 10: Asymptotic subsystem temperature T_{sub} as a function of the bath temperature T_{bath} for two different drags: $A = 0.1$ (red circles) and $A = 1.5$ (blue crosses) corresponding respectively to a weak and strong coupling. The dashed line corresponds to the ideal case $T_{\text{sub}} = T_{\text{bath}}$.

In Fig. 10, we compare the temperature actually reached by our subsystem T_{sub} to the bath temperature T_{bath} used as input of the noise. For a large range of temperatures and independently of the drag A and initial state, we observe that $T_{\text{sub}} \simeq T_{\text{bath}}$ and that the asymptotic distributions of the weights are Boltzmannian. One can thus conclude that the subsystem correctly thermalises when one uses the white quantum noise (2.9) with (2.10).

The total uncertainty on the asymptotic values, for a statistic of a few thousands of realisations, grows with the temperature from $\sim 2\%$ at $T_{\text{bath}} = 0.1$ to $\sim 10\%$ at $T_{\text{bath}} = 5$. Indeed, a higher temperature implies larger wavefunction oscillations along the space axis, which implies larger weight oscillations at each noise realisation and for the mixed state observables. An additional averaging over a time range $\Delta t'$ once the equilibrium reached, leads to more reliable results whose accuracy then follows the common statistical law $\propto 1/\sqrt{n_{\text{stat}} \times \Delta t'}$. When $T_{\text{bath}} \ll 1$, some light “saturation” effects are observed for really small weights ($\lesssim 10^{-8}$). They are most probably due to numerical issues, associated for instance to the discretization scheme or the spectrum approximation (due to the “infinite walls” at the grid limits [42]).

We have therefore generalised the analytic results obtained in Sec. III A 1 with an initial Gaussian wavepacket to some other initial states. We can thus conjecture that the SL equation, with a harmonic external potential and the white quantum noise (2.9) and (2.10), universally leads to the thermal equilibrium of statistical mechanics. Moreover, though only expected at the weak coupling limit (as explained in the introduction), it is also reached in the intermediate and strong regimes. Finally, the observed behaviour fits Senitzky’s point of view that initial correlations should be suppressed and replaced by some universal thermal correlations.

B. Linear potential

As explained in Sec. II B 1, the white quantum noise (2.9) and (2.10) was initially derived for a harmonic potential. In this section, we test its ability to be extended to other types of potentials through the example of the linear potential $V_{\text{ext}} = 1/2 |x|$. In the white quantum noise expression (2.10), we set E_0 to the value 0.509 equal to the ground state energy.

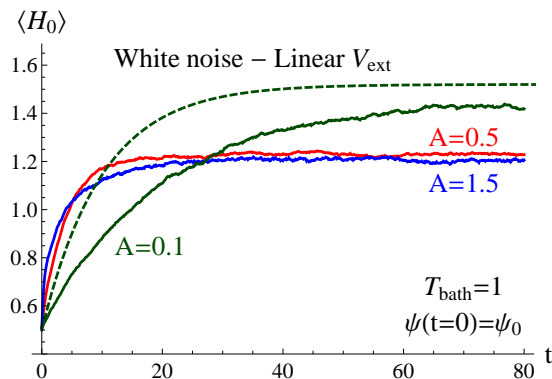


FIG. 11: Numerical average energy $\langle H_0 \rangle$ evolutions for different drags A (solid curves) and the theoretical evolution given by (3.5) with $\{T_{\text{bath}} = 1, \langle H_0 \rangle(t \rightarrow \infty) = 1.52, A = 0.1\}$ (dashed curve).

As shown in Fig. 11, the asymptotic value of the $\langle H_0 \rangle$ average energy exhibits a strong A -dependence and is not equal to

$$\langle H_0 \rangle(t \rightarrow \infty) = \frac{\sum_i E_i e^{-E_i/T_{\text{bath}}}}{\sum_i e^{-E_i/T_{\text{bath}}}} \simeq 1.52, \quad (3.6)$$

as should be expected. At small drags, the average energy evolutions are nevertheless in good agreement with the exponential rate (3.5) when one takes the measured $\langle H_0 \rangle(t \rightarrow \infty)$ and effective $A_{\text{eff}} \simeq A/2$ values.

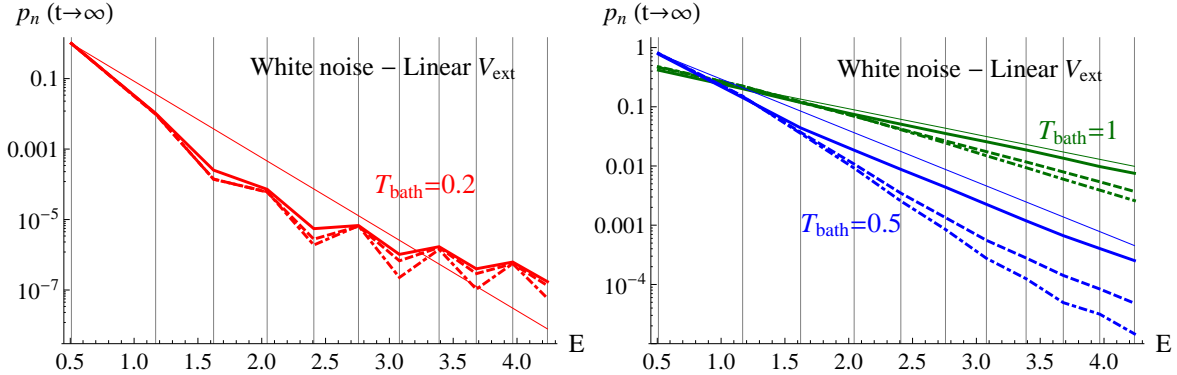


FIG. 12: The asymptotic distributions of the eigenstate weights $p_{n=0,\dots,10}$ (joined by lines) function of the eigenenergies $E_{n=0,\dots,10}$ (vertical lines), obtained with different drags $A = 0.1$ (solid lines), $A = 0.5$ (dashed lines) and $A = 1.5$ (dot-dashed lines) and temperatures $T_{\text{bath}} = 0.2$ (left), $T_{\text{bath}} = 0.5$ and 1 (right). They are compared to the corresponding “ideal” Boltzmann distributions $\propto e^{-E/T_{\text{bath}}}$ (thin lines).

Independent of the initial state, the asymptotic distributions of the weights $p_{n=0,\dots,10}$ are close to the Boltzmann distributions $\propto e^{-E/T_{\text{bath}}}$ only when $1 \lesssim T_{\text{bath}} \lesssim 2$ at weak couplings (see Fig. 12). At low temperatures strong discrepancies are observed: the higher excited states exceed the Boltzmann law, exhibit an alternating pattern and saturate at low weights. Moreover, a dependence on the drag value is observed from the 2nd (4th) excited state at low (medium) temperatures. The latter explains the $\langle H_0 \rangle$ dependence on the drag observed in Fig. 11: a smaller drag is observed to generate higher populations for the excited eigenstates and thus a higher average energy.

These discrepancies make the determination of T_{sub} uncertain. Here, T_{sub} will be estimated by tracing the effective Boltzmann lines $\propto e^{-E/T_{\text{sub}}}$ between the two first weights (p_0 and p_1) as a minimum. The latter are indeed more interesting phenomenologically and less subject to numerical uncertainties. The numbers of low lying eigenstates which are then close to the effective Boltzmann lines are summed up in Tab. I. The evaluation of T_{sub} vs. T_{bath} , showed in Fig. 13, exhibits clear discrepancies to the “ideal” $T_{\text{sub}} = T_{\text{bath}}$ line at low and high temperatures and for any drag value. At high temperatures our accuracy on T_{sub} is low due to a very large time required to reach the asymptotes and a large uncertainty as in Sec. III A 4 (e.g. for $A = 0.1$, $T_{\text{sub}} \in [4.3, 8.3]$ with an average of ~ 6.5).

In view of these elements, we conclude that the white quantum noise (2.9) is not quite suitable to obtain an acceptable thermal equilibrium (in the sense of $p_n \propto e^{-E_n/T_{\text{bath}}}$)

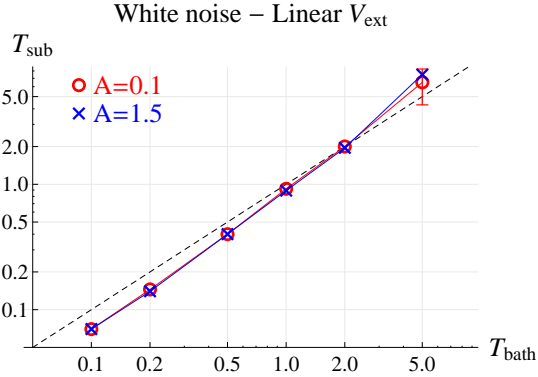


FIG. 13: Asymptotic subsystem temperature T_{sub} as a function of the bath temperature T_{bath} for two different drags $A = 0.1$ (red circles) and $A = 1.5$ (blue crosses) corresponding respectively to weak and strong couplings. The dashed line corresponds to the ideal case $T_{\text{sub}} = T_{\text{bath}}$.

— Number of weights close to $\propto e^{-E/T_{\text{sub}}}$? —			
$T_{\text{bath}} \setminus$ Coupling	Weak	Intermediate	Strong
Low ($T_{\text{bath}} < 0.5$)	3	2	2
Medium ($0.5 < T_{\text{bath}} < 2$)	5	5	4
High ($T_{\text{bath}} > 2$)	10	9	8

TABLE I: Approximate number of weights close to the corresponding Boltzmannian $\propto e^{-E/T_{\text{sub}}}$. One can consider the agreement to be poor from 2 to 4 weights, good from 5 to 7 and very good from 8 to 11.

with other external potentials than the harmonic one. Nevertheless, if one is interested in a limited number of low lying eigenstates (see Tab. I), this formalism could be used for phenomenological purposes by performing a rescaling in the noise expression (2.10): either by changing the value of E_0 (to 0.33 here) or by choosing the input T_{bath} such as to obtain the desired $T_{\text{sub}} = T_{\text{bath}}$. Conversely, this study confirms the very specific nature of the harmonic potential upon which general conclusions should not be drawn as regards the applicability of any scheme aiming at describing the thermalisation of quantum subsystem.

IV. EQUILIBRATION WITH A COLORED QUANTUM NOISE

We now use the colored quantum noise (2.12) to study the SL equation ability to bring a subsystem to the thermal equilibrium of statistical mechanics. Whereas the white quantum noise (2.9) led to an uncorrelated stochastic force, the colored quantum noise (2.12) gives a stochastic force with a strong temperature dependence of its correlation time. The latter becomes really large at low temperatures ($\propto 1/T$) and the Brownian hierarchy/weak coupling limit - the typical relaxation time ($\propto 1/A$) should be much larger than the stochastic force correlation time - is broken when $A \gtrsim T$.

A. Harmonic potential

The evolution of the $\langle H_0 \rangle$ average energy is close to the one obtained with the white quantum noise (Fig. 7) and fits Senitzky’s law (3.5) in the weak coupling limit. The evolutions of the eigenstate weights are also close to the ones obtained with the white quantum noise (Fig. 8). As illustrated in Fig. 14, the asymptotic distributions of the weights are Boltzmannian independently of the drag A and initial state, and all the observations made in Sec. III A 4 apply here too. In Fig. 15, we compare the temperature actually reached by our subsystem T_{sub} to the bath temperature T_{bath} used as input of the noise. When $T_{\text{bath}} \gtrsim 0.5$, the subsystem correctly thermalises in a good approximation (we note a light drag dependence: the larger A the smaller T_{sub}). At lower temperatures, some important discrepancies (T_{sub} “saturates”) appear when $A \gtrsim T_{\text{bath}}$. These weight discrepancies must therefore originate from the Brownian hierarchy breaking as described above.

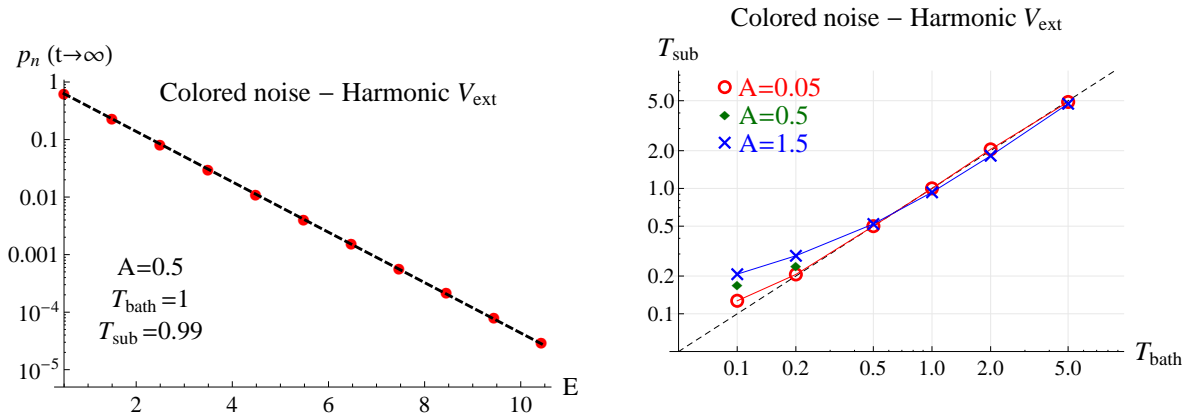


FIG. 14: The asymptotic distribution of the eigenstate weights $p_{n=0,\dots,10}$ (red dots), obtained with $\{A = 0.5, T_{\text{bath}} = 1\}$, function of the eigenenergies $E_{n=0,\dots,10}$, in comparison to the Boltzmann distribution ($\propto e^{-E/T_{\text{sub}}}$) at $T_{\text{sub}} = 0.99$ (dashed line).

FIG. 15: Asymptotic subsystem temperature T_{sub} as a function of the bath temperature T_{bath} for three different drags: $A = 0.05$ (red circles), $A = 0.5$ (green diamonds) and $A = 1.5$ (blue crosses) corresponding respectively to a weak, intermediate and strong coupling. The dashed line corresponds to the ideal case $T_{\text{sub}} = T_{\text{bath}}$.

B. Linear potential

Unlike the white quantum noise, the colored quantum noise (2.12) was derived without assumptions on the external potential. In this section, we test its ability to be extended to other potentials through the example of the linear potential.

As shown in Fig. 16 (left), the $\langle H_0 \rangle$ average energies are similar to the ones obtained with the white quantum noise (Fig. 11). As shown in Fig. 17, the asymptotic distributions of the weights are observed to be independent of the initial state and close to the Boltzmann distributions $\propto e^{-E/T_{\text{bath}}}$ for a limited numbers of low lying eigenstates at the weak coupling limit and at strong couplings when $T_{\text{bath}} \gtrsim A$. At intermediate couplings, the distributions are observed to be “perfectly” Boltzmannian when $T_{\text{bath}} \gtrsim A$. When $T_{\text{bath}} < 0.2$, we observe a similar alternating pattern behaviour than in the white quantum noise case (see Fig. 12)

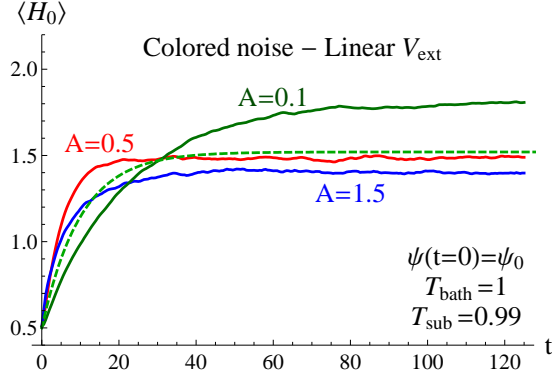


FIG. 16: Same as Fig. 11 for the case of the colored quantum noise.

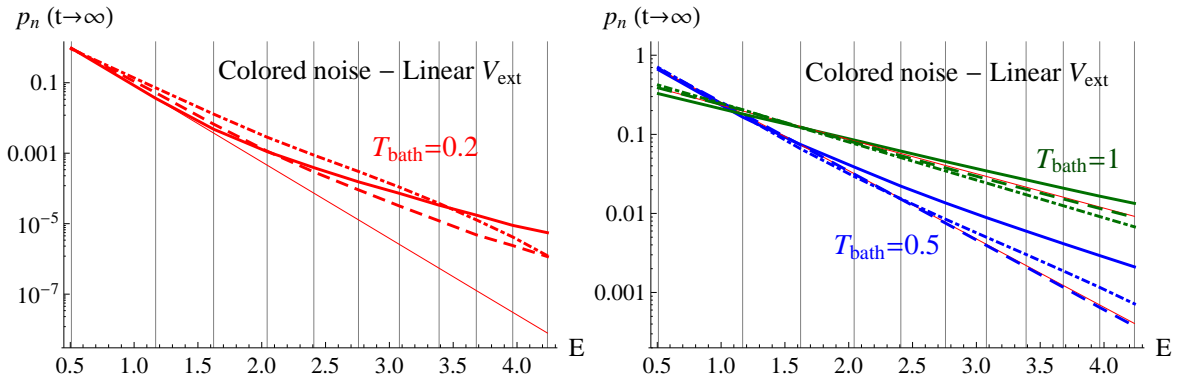


FIG. 17: Same as Fig. 12 for the case of the colored quantum noise.

with however lighter oscillations. Despite these discrepancies, the relation T_{sub} vs. T_{bath} (Fig. 18), obtained by focusing on the lowest excited states, is interestingly close to the one obtained with the harmonic potential, with the exception of the high temperature regime where one naturally recovers the white quantum noise results ($T_{\text{sub}} > T_{\text{bath}}$). These observations confirm the rather “universal” nature of the colored quantum noise (2.12), which might thus be combined with a wider class of potentials and used in a good approximation for thermalisation studies in the weak coupling case.

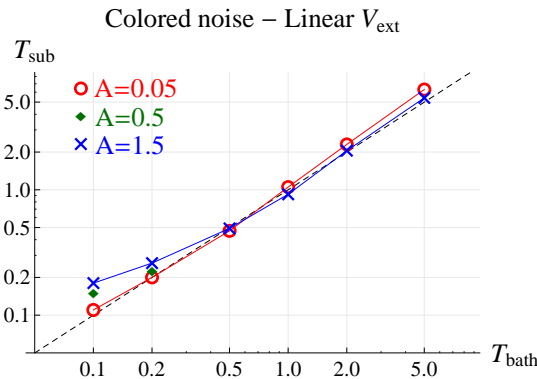


FIG. 18: Same as Fig. 15 for the case of the linear external potential.

V. DISCUSSION AND CONCLUSION

For the purpose of finding an effective formalism suitable to phenomenological applications of open quantum systems, we have focused on the Schrödinger-Langevin (SL) eq. (1.2). Its nonlinear friction term is commonly believed to maintain the stationarity of the excited states of the uncoupled Hamiltonian H_0 . We have shown in Sec. II A that the Madelung/polar transformation of the wavefunction leads to a nonzero damping for these states. In this way, we have reconciled the SL equation with the intuitive expectation that the dissipation process should act on any state in order to bring the subsystem to its ground state.

We have then focused on the solutions of the SL equation with two different noise operators taken as c-numbers: the white quantum noise (2.9, 2.10) - which has been derived by Senitzky [1] and subtracted by its term of ground state fluctuations - and the colored quantum noise (2.12) derived by Ford, Kac and Mazur [12]. When the subsystem undergoes a harmonic potential, the SL equation has demonstrated its ability to bring any initial state to the thermal equilibrium of statistical mechanics (i.e. Boltzmann distributions of the uncoupled subsystem energy states) in the weak coupling limit with either noise, confirming the assumption made by Messer [41]. Though only expected at this limit (as explained in the introduction), the intermediate and strong regimes have also led to the same equilibrium with the white quantum noise and partially with the colored quantum noise. For this case, some disagreements between the subsystem temperature T_{sub} and the bath temperature T_{bath} (input of the noise) have been observed at low temperatures and attributed to the breaking of the Brownian hierarchy. When the subsystem is submitted to a linear potential, non-Boltzmannian behaviours and stronger drag dependences have been observed at low and medium temperatures for both kind of noises. Nevertheless, the colored quantum noise has led to better results in the sense of statistical mechanics, confirming its rather universal nature. It should thus be used preferentially, especially at low temperatures (provided the Brownian hierarchy is preserved). If one focuses on phenomenological applications where only the lower states are considered (especially at low temperatures), one can rectify the observed differences between T_{sub} and T_{bath} by choosing an effective heat-bath temperature \tilde{T}_{bath} such as to reach the desired subsystem temperature $T_{\text{sub}} = T_{\text{bath}}$. It just requires the proper knowledge of the $T_{\text{sub}}(T_{\text{bath}})$ function as displayed in Fig. 13 and 18.

Though one has to adapt this rescaling at each situation, the SL equation can thus be used, in a good approximation, as an effective open quantum system formalism in phenomenological applications (such as ions transport, thermalisation of quarkonia in a quark-gluon plasma, of nucleons in a nucleus, of atoms in a magnetic trap...). As shown in our work, dealing with the full hierarchy of states in the general case requires a more refined quantum treatment of the subsystem interactions with the heat bath.

It should be noted that our analysis relies on the hypothesis that the asymptotic distribution of subsystem-eigenstates weights p_n must be Boltzmannian whatever the potential and the coupling strength to the rest of the system (the heat bath). To our knowledge, such an assumption has not been universally established from fundamental principles (i.e. starting from the distribution of the full-system eigenstates and tracing out the heat-bath degrees of freedom) and should be considered more thoroughly in future studies as it could partially alter our conclusions.

Appendix A: White quantum noise and Boltzmann distributions

When the subsystem external potential is harmonic, we showed in Sec. III A 1 that Gaussian wavepackets reduces asymptotically to the a coherent state with a width a corresponding to the ground state. Therefore, for asymptotic times the wavefunction writes,

$$\psi \propto e^{-\frac{(x-x_{\text{cl}}(t))^2}{2a^2} + ip_{\text{cl}}(t)x}, \quad (\text{A1})$$

where the square width is $a^2 = \frac{1}{m\omega_0}$. We would like to know what is the weight of the different H_0 eigenstates

$$\psi_n = \frac{H_n(\xi)e^{-\frac{\xi^2}{2}}}{\sqrt{2^n n! \sqrt{\pi}}}, \quad (\text{A2})$$

where $\xi = \frac{x}{a}$. We first reformulate (A1) as

$$\psi \propto e^{-\frac{\xi^2}{2} + 2\mu\xi - \frac{(x_{\text{cl}}/a)^2}{2}}, \quad (\text{A3})$$

where we have set $\mu = \frac{x_{\text{cl}}}{a} + ip_{\text{cl}}a$. Using the identity

$$e^{2\mu\xi - \mu^2} = \sum_{n=0}^{+\infty} \frac{\mu^n}{n!} H_n(\xi), \quad (\text{A4})$$

then yields

$$\psi \propto e^{-\frac{(x_{\text{cl}}/a)^2}{4} - \frac{(p_{\text{cl}}a)^2}{4} + i\frac{p_{\text{cl}}x_{\text{cl}}}{2}} \sum_{n=0}^{+\infty} \frac{\sqrt{2^n} \mu^n}{\sqrt{n!}} \psi_n(\xi). \quad (\text{A5})$$

We thus deduce that the eigenstate weight $p_n(x_{\text{cl}}, p_{\text{cl}})$ for a given realisation of the stochastic noise is given by

$$p_n(x_{\text{cl}}, p_{\text{cl}}) \propto \frac{2^n |\mu|^{2n}}{n!} e^{-\frac{(x_{\text{cl}}/a)^2}{2} - \frac{(p_{\text{cl}}a)^2}{2}} \propto \frac{((x_{\text{cl}}/a)^2 + (p_{\text{cl}}a)^2)^n}{2^n n!} e^{-\frac{(x_{\text{cl}}/a)^2}{2} - \frac{(p_{\text{cl}}a)^2}{2}} \quad (\text{A6})$$

and one has exactly $\sum p_n = 1$. In Sec. III A 1, we showed that the position x_{cl} and momentum p_{cl} centroids satisfy the classical stochastic equation of motion (3.3). When the stochastic force correlation is of the form $\langle F_R(t)F_R(t+\tau) \rangle = B\delta(\tau)$ (white noise) it is known that the distribution of the trajectories $(x_{\text{cl}}, p_{\text{cl}})$ is

$$W(x_{\text{cl}}, p_{\text{cl}}) \propto e^{-\frac{\frac{m\omega_0^2 x_{\text{cl}}^2}{2} + \frac{p_{\text{cl}}^2}{2m}}{kT_{\text{cl}}}}, \quad (\text{A7})$$

where $T_{\text{cl}} := \frac{B}{2mA}$, A is the drag and B the force autocorrelation. The eigenstate weight, averaged over the fluctuations, will then be given by

$$p_n = \int W(x_{\text{cl}}, p_{\text{cl}}) p_n(x_{\text{cl}}, p_{\text{cl}}) dx_{\text{cl}} dp_{\text{cl}}. \quad (\text{A8})$$

To determine (A8), we use the relation

$$p_n(x_{\text{cl}}, p_{\text{cl}}) = \frac{(-1)^n}{n!} \frac{\partial^n}{\partial \eta^n} e^{-\eta \left(\frac{(x_{\text{cl}}/a)^2}{2} + \frac{(p_{\text{cl}}/a)^2}{2} \right)} \Bigg|_{\eta=1}. \quad (\text{A9})$$

After some trivial integration on x_{cl} and p_{cl} , one gets that

$$\int W(x_{\text{cl}}, p_{\text{cl}}) e^{-\eta \left(\frac{(x_{\text{cl}}/a)^2}{2} + \frac{(p_{\text{cl}}/a)^2}{2} \right)} dx_{\text{cl}} dp_{\text{cl}} = \frac{\frac{\hbar\omega_0}{kT_{\text{cl}}}}{\eta + \frac{\hbar\omega_0}{kT_{\text{cl}}}}, \quad (\text{A10})$$

where the numerators guarantees that for $\eta = 0$, one has $\int W(x_{\text{cl}}, p_{\text{cl}}) dx_{\text{cl}} dp_{\text{cl}} = 1$. Differentiating n times (A10) with respect to η yields

$$p_n = \frac{\frac{\hbar\omega_0}{kT_{\text{cl}}}}{\left(1 + \frac{\hbar\omega_0}{kT_{\text{cl}}}\right)^n} \quad (\text{A11})$$

We thus have

$$p_n \propto e^{-n \ln\left(1 + \frac{\hbar\omega_0}{kT_{\text{cl}}}\right)}. \quad (\text{A12})$$

Setting

$$\ln\left(1 + \frac{\hbar\omega_0}{kT_{\text{cl}}}\right) = \frac{\hbar\omega_0}{kT_{\text{sub}}} \Leftrightarrow kT_{\text{cl}} = \frac{\hbar\omega_0}{e^{\frac{\hbar\omega_0}{kT_{\text{sub}}}} - 1}, \quad (\text{A13})$$

one obtains $p_n \propto e^{-n \frac{\hbar\omega_0}{kT_{\text{sub}}}}$ which shows that the distribution of states follows a Boltzmann distribution with a temperature T_{sub} . Recalling the expression of T_{cl} , one gets the condition relating A , B and T_{sub} :

$$\frac{B}{2mA} = \frac{\hbar\omega_0}{2} \left[\coth\left(\frac{\hbar\omega_0}{2kT_{\text{sub}}}\right) - 1 \right], \quad (\text{A14})$$

which is the relation (2.10) for the white quantum noise and shows that $T_{\text{sub}} = T_{\text{bath}}$ the bath temperature. Reciprocally, we have proven that the distribution of the state weights is Boltzmannian if one uses a white quantum noise with the relation (2.10). This reasoning can be easily extended to three dimensions.

Acknowledgments

We are grateful for support from TOGETHER project Région Pays de la Loire.

-
- [1] I. R. Senitzky, Phys. Rev. **119**, 670 (1960); **124**, 642 (1961).
 [2] J. H. Weiner and R. E. Forman, Phys. Rev. B **10**, 325 (1974).

- [3] S. Bhattacharya, S. Dutta and S. Roy, *Journal of Modern Physics* **2**, 231-235 (2011).
- [4] J. J. Degman, D. B. Coyle and R. B. Kay, *IEEE J. Quantum Electron.* **34** (5), 887-899 (1998).
- [5] D. H. E. Gross and H. Kalinowski, *Physics Reports* **45** (3), 176210 (1978).
- [6] Y. Hamdouni, *J. Phys. G*, **37** (12), 125106 (2010).
- [7] K. Yasue, *Annals Phys.* **114**, 479-496 (1978).
- [8] M. A. Nielsen and I. L. Chuang, *Quantum Computation and Quantum Information*, (Cambridge University Press, Cambridge, 2000).
- [9] L. Henriot, Z. Ristivojevic, P. P. Orth, K. Le Hur, *Phys.Rev. A* **90**, 023820 (2014).
- [10] G. Lindblad, *Rept. Math. Phys.* **10**, 393 (1976).
- [11] M. S. Wartak, *J. Phys. A: Math. Gen.* **22** (9), L361 (1989).
- [12] G. W. Ford, M. Kac, and P. Mazur, *J. Math. Phys.* **6**, 504 (1965).
- [13] A. O. Caldeira and A. J. Leggett, *Physica A* **121**, 587 (1983).
- [14] R. Benguria and M. Kac, *Phys. Rev. Lett.* **46**, 1 (1981).
- [15] E. Nelson, *Phys. Rev.* **150**, 1079 (1966).
- [16] M. Razavy, *Z. Physik B* **26**, 201 (1977).
- [17] H. Dekker, *Phys. Rev. A* **16**, 21262134 (1977).
- [18] P. Caldirola, *Nuevo Cimento* **18**, 393 (1941); E. Kanai, *Prog. Theor. Phys.* **3**, 440 (1948).
- [19] I. R. Svin'in, *Teor. Mat. Fiz.* **22**, 107 (1975).
- [20] V. E. Tarasov, *Theor. Math. Phys.* **100**, 1100 (1994).
- [21] A. O. Bolivar *Phys. Rev. A* **58**, 4330 (1998).
- [22] H. Dekker, *Z. Physik B* **21**, 295 (1975); H. Dekker, *Physica A* **95**, 311 (1979).
- [23] K. K. Kan and J. J. Griffin, *Phys. Lett. B* **50** (2), 241243 (1974).
- [24] S. Garashchuk, V. Dixit, B. Gu and J. Mazzuca, *J. Chem. Phys.* **138**, 054107 (2013).
- [25] M. D. Kostin, *J. Chem. Phys.* **57**, 3589 (1972).
- [26] H. D. Doebner, G. A. Goldin and P. Nattermann, *J. Math. Phys.* **40**, 49 (1999).
- [27] R. J. Wysocki, *Phys. Rev. A*, **61**, 022104 (2000).
- [28] T. Fulop and S. D. Katz, [arXiv: quant-ph/9806067] (1998).
- [29] P. Ruggiero and M. Zannetti, *La Rivista Del Nuovo Cimento Series 3*, **8** (5), 1-47 (1985).
- [30] A.L. Sanin and A.A. Smirnovsky, *Materials Physics and Mechanics*, **20**, 98-105 (2014).
- [31] H. Dekker, *Physics Reports*, **80** (1), 1110 (1981).
- [32] J. L. López and J. Montejo-Gámez, *J. Math. Anal. Appl.* **383**, 365-378 (2011).
- [33] P. Bargueño and S. Miret-Artés, *Ann. Phys.* **346**, 5965 (2014).
- [34] J. D. Immele, K. K. Kan and J. J. Griffin, *Nucl. Phys. A* **241**, 47 (1975).
- [35] R. W. Hasse, *J. Math. Phys.* **16**, 2005 (1975).
- [36] B. S. Skargerstam, *Phys. Lett. B* **58**, 21 (1975).
- [37] L. Brüll and H. Lange, *J. Math. Phys.* **25**, 786790 (1984).
- [38] D. de Falco and D. Tamascelli, *Phys. Rev. A* **79**, 012315 (2009).
- [39] T. Wells, J. D. Immele, K. K. Kan and J. J. Griffin, *Bull. Am. Phys. Soc.* **19**, 527 (1974).
- [40] M. Razavy, *Can. J. Phys.* **56**, 311 (1978).
- [41] J. Messer, *Acta Phys. Austriaca* **50**, 75-91 (1979).
- [42] A.L. Sanin and A.A. Smirnovsky, *Phys. Lett. A* **372**, 21-27 (2007).
- [43] P. Van and T. Fulop, *Phys. Lett. A* **323** (5-6), 374-381 (2004).
- [44] V. E. Tarasov, *Phys. Lett. A* **299**, 173-178 (2002).
- [45] X.L. Li, G.W. Ford and R.F. O'Connell, *Phys. Rev. E* **51** (5), 5169-5171 (1995).
- [46] C. Gardiner and P. Zoller, *Quantum Noise, A Handbook of Markovian and Non-Markovian Quantum Stochastic Methods with Applications to Quantum Optics*, (Springer, Berlin, 2000),

chap. 3.6 and chap. 1.2.

- [47] R. H. Koch, D. J. van Harlingen and J. Clarke, Phys. Rev. Lett. **47** (17), 1216 (1981).
- [48] R. H. Koch, D. J. van Harlingen, and J. Clarke, Phys. Rev. Lett. **45**, 2132 (1980).
- [49] K. L. Sebastian, Chem. Phys. Lett. **81**, 14 (1981).
- [50] A. Schmid, J. Low Temp. Phys. **49**, 608 (1982).
- [51] H. Metiu and G. Schön, Phys. Rev. Lett. **53**, 13 (1984).
- [52] D. Banerjee, B. Chandra Bag, S. Kumar Banik, D. Shankar Ray, [arXiv: cond-mat/0303059] (2003).